Time-Domain-Based Modeling of Carrier Transport in Lateral p-i-n Photodiode

G. Suzuki, K. Konno, D. Navarro, N. Sadachika Y. Mizukane, O. Matsushima, T. Ezaki, M. Miura-Mattausch and S. Yokoyama

Graduate School of Advanced Sciences of Matter, Hiroshima University, Higashi-Hiroshima 739-8530, Japan.

Abstract

Carrier transport in a lateral p-i-n photodiode (PD) has been fully-described analytically in time domain by adopting a coordinate transformation where carriers are assumed to be fixed in a coordinate system. Our model correctly predicts the measured delayed response of a PD in a 100ps-Gaussian pulse, which is not observed in stationary and constant electric field approximations. The PD delay is reflected in the transient characteristics of an inverter circuit with the PD response used as input.

1 Introduction

Advanced LSI in which optical interconnects is implemented [1], i.e., optoelectronic integrated circuits (OEICs) is expected to show great performance for high speed operation. Such OEICs are composed of light emitting devices, optical waveguide, and photodetectors. In order to fully utilize the optical interconnects in LSI, development of models for optoelectronic devices is prerequisite for circuit design of OEICs.

In this paper, we model the carrier transport in a lateral p-i-n PD, which is used as a photodetector in LSI. Our time-domain-based model is particularly useful for time-domain-based circuit simulators like SPICE (see Ref. [2] for modeling in frequency domain).

2 Formulation of Carrier Transport

Instead of a realistic structure of a lateral p-i-n PD as shown in Fig. 1(a), we consider a simplified structure shown in Fig. 1(b) to formulate our model. Here, we assume: (i) homogeneous irradiation only on the intrinsic region, (ii) deep n^+ and p^+ region compared with the light penetration depth, (iii) negligible y-component of the electric field $\vec{E} = (E_x, 0)$, where E_x is in general a function of y, in the intrinsic region, (iv) negligible change of the electric field due to incident light (see Ref. [3] for high intensity illumination). From the above assumptions, the carrier trajectory is restricted in one dimension. The equations governing the carrier dynamics are

$$\partial_t n(x,y,t) - q^{-1}\partial_x J_{x,n}(x,y,t) = G_n(y,t), \quad \partial_t p(x,y,t) - q^{-1}\partial_x J_{x,p}(x,y,t) = G_p(y,t). \tag{1}$$

Here, $J_{x,n} = q\mu_n(E_x)E_x(y)n(x,y,t)$, $J_{x,p} = q\mu_p(E_x)E_x(y)p(x,y,t)$, and $G_n(y,t) = G_p(y,t) = \alpha e^{-\alpha y}\phi(t)$, where n and p are the charge density of electrons and holes respectively, $J_{x,n}$ and $J_{x,p}$ are the current density, $G_{n,p}$ is the carrier generation rate, $\mu_{n,p}$ is the mobility of carriers, α is the absorption coefficient, and ϕ is the photon flux.

We apply the following coordinate transformation to the above differential equations: $\xi_{n,p} = (t + x/v_{n,p})/2$, $\eta_{n,p} = (t - x/v_{n,p})$, where $v_n = -\mu_n E_x$, $v_p = \mu_p E_x$. First-order differential equations with respect to ξ, which can easily be solved, are derived. We obtain

$$I(t) = \alpha q W \int_0^\infty dy \int_{t-L/|v_p(y)|}^{t} dt' \mu_p(E_x)|E_x(y)|e^{-\alpha y}\phi(t'), \tag{2}$$

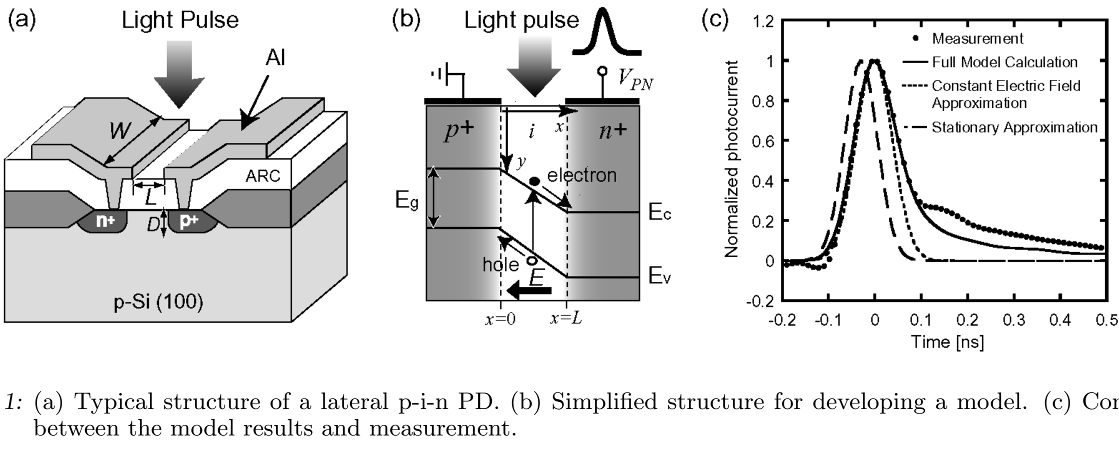

Figure 1: (a) Typical structure of a lateral p-i-n PD. (b) Simplified structure for developing a model. (c) Comparison between the model results and measurement.

where L is the length of intrinsic region, and W is the width of the device. Since the slower carriers, i.e., holes determine the operation speed of the PD, we concentrated on the parameters of hole. If the change of $\phi(t)$ during the time interval $\Delta t \sim L/|v_p|$ is very small, then we have $I(t) \simeq qLW\phi(t)$. On the other hand, when the electric field is almost constant, i.e., $|E_x(y)| = E_0$ down to the light penetration depth, we have $I(t) \simeq q\mu_p E_0 \int_{t-\Delta t}^{t} \phi(t')dt'$. Estimation without approximations is obtained from numerical calculations of Eq. (2). These formulae are useful for describing non-stationary features of carrier transport.

3 Comparison with Measurement

We have compared the photocurrent calculation results of our model with measurement, which is shown in Fig. 1(c). For this purpose, we fabricated a silicon lateral p-i-n PD as shown in Fig. 1(a), where the device dimensions are $L = 2\mu$m, $D = 0.5\mu$m, and the doping concentration is given by $n^+ \sim 10^{20}$cm^{-3}, $p^+ \sim 10^{20}$cm^{-3}, substrate $\sim 10^{15}$cm^{-3}. A Gaussian-pulsed laser with wavelength of 532nm and full-width at half maximum of $\sim$ 100ps is used as the input light pulse. The applied bias voltage is $V_{PN} = 2$V. The photocurrent is normalized with respect to the peak value. The stationary approximation and the constant electric field approximation predict the general profile of the measured pulse but the end tail can not be reproduced. The full calculation successfully reproduces the end tail. In the full calculation, we assumed the electric field $E_x(y) = E_0 \exp\left(-y^2/D^2\right)$, where $E_0 \sim V_{PN}/L$. This expression approximately reproduces the electric field configuration derived from a 2-dimensional device simulator. The remaining difference is considered to be due to the carriers generated in the n^+ or p^+ region, which cause slow response because the carrier transport is governed by diffusion.

4 Application to Circuit Simulation

We consider merging the current formulae for the PD with a time-domain-based circuit simulator, e.g., HSPICE. We adopt a test circuit given in Fig. 2(b), where the PD output current is amplified by the op-amp to modulate the PD current and convert to voltage input for the inverter circuit. The PD is implemented by an equivalent circuit shown in Fig. 2(a), where the independent current source is described by the PD current formulae. The results are given in Fig. 2(c). The delay that is inherent in the full-model calculation is exhibited in the inverter output.

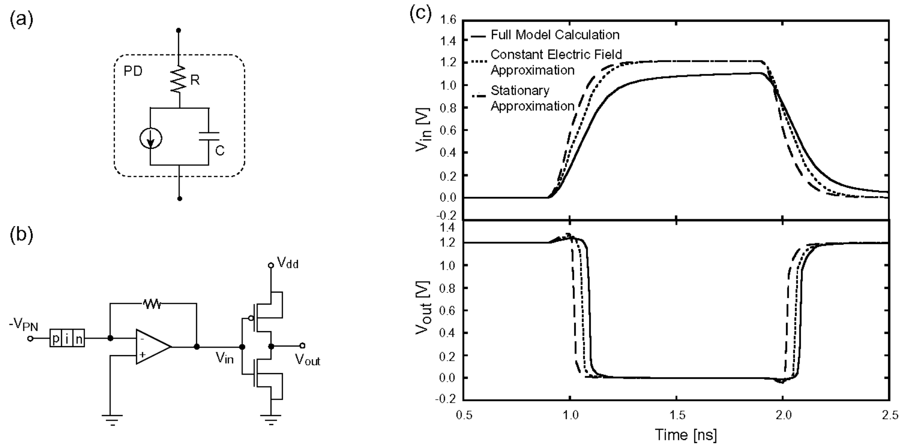

Figure 2: (a) Equivalent circuit of the PD, which is merged with circuits. (b) A Test circuit. (c) Input voltage $V_{\rm in}$ and Output voltage $V_{\rm out}$ as a function of time.

5 Conclusion

We have developed a time-domain description of photoresponse of the lateral p-i-n photodiode, which takes into account the non-stationary features of carrier transport beyond cutoff frequency. We also demonstrated merging of the PD model with the circuit simulator HSPICE. Our model is very useful for circuit design of LSI having optical interconnects.

References

[1] L. C. Kimerling, Appl. Surf. Sci., **159-160**, 8 (2000).

[2] K. Konno et al., J. Appl. Phys. **96**, 3839 (2004); K. Konno et al., J. J. Appl. Phys. **44**, (in press).

[3] O. Matsushima et al., Semicond. Sci. Technol. **19**, S185 (2004); K. Konno et al., Appl. Phys. Lett. **84**, 1398 (2004).

Time-Domain-Based Modeling of Carrier Transport in Lateral p-i-n Photodiode

G. Suzuki, K. Konno, D. Navarro, N. Sadachika, Y. Mizukane, O. Matsushima, T. Ezaki, M. Miura-Mattausch and S. Yokoyama

Graduate School of Advanced Sciences of Matter, Hiroshima University

I. Introduction

Conventional metal interconnect raises problems for advanced LSI circuits.

Problems:

- Propagation delay
- Power consumption
- Size

Optical interconnect is an attractive alternate.

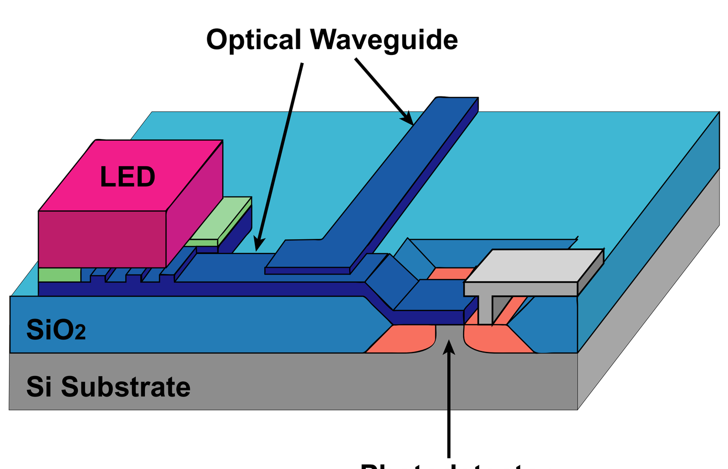

Optoelectronic Integrated Circuit (OEIC)

Circuit simulation of optoelectronic integrated circuits (OEICs) is necessary.

II. Objectives

To develop a lateral p-i-n photodiode for circuit simulation.

Frequency-Domain Approach ⇨ Konno et al., SSDM (2004)

- Frequency-Domain-Based Circuit Simulator (Harmonic Balance Simulator): Compatible
- Time-Domain-Based Circuit Simulator (SPICE): Compatible via FFT

Time-Domain Approach ⇨ This work

- Time-Domain-Based Circuit Simulator (SPICE): Compatible

For implementation in SPICE-type simulators, the time-domain approach is desirable.

III. Lateral p-i-n Photodiode

Lateral p-i-n photodiode enables high responsivity and high speed operation even for long wavelength light pulse.

Direction:

Carrier flow ⊥ Light penetration

Related literature:

Hanafusa et al. (1993); He et al. (1994); Ghioni et al. (1996); Schow et al. (1999); Yang et al. (2002), etc.

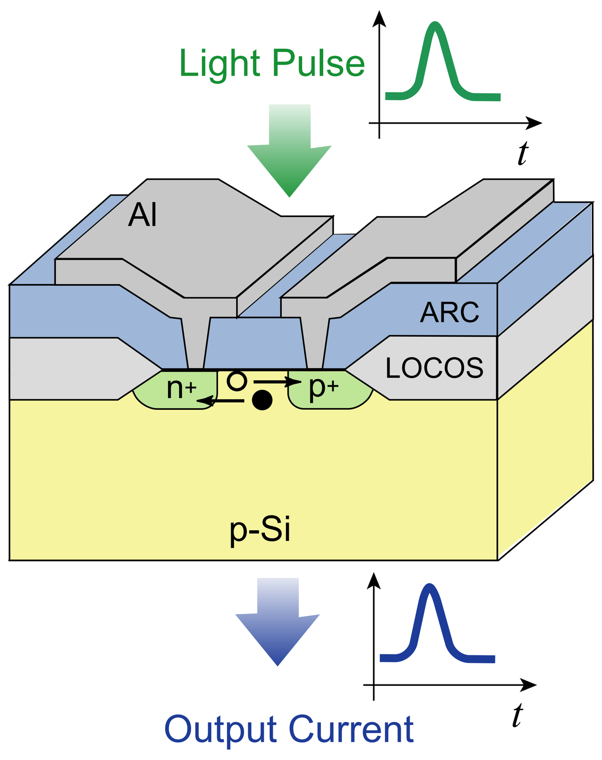

IV. How to Model Photodiode

Assumptions:

1. Homogeneous irradiation only in the i-region
2. Deep p^+ and n^+ region compared with the light penetration depth
3. Constant electric field E_x in the x-direction and negligible y-component of the electric field: $E=(E_x,E_y)=(E_0,0)$
4. Negligible change of the electric field due to the incident light pulse

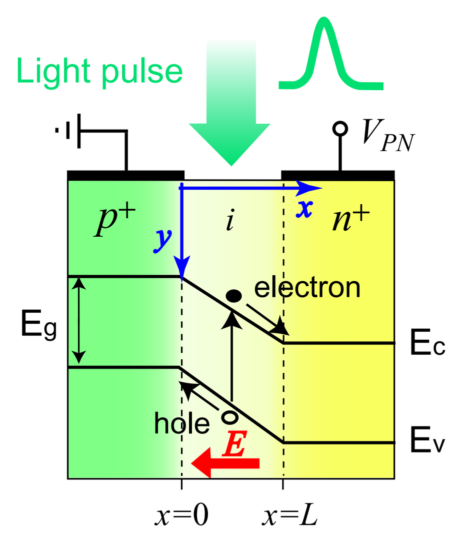

V. Time-Domain-Based Modeling

Continuity equation: $\frac{\partial n(x,y,t)}{\partial t} - \frac{1}{q}\frac{\partial J(x,y,t)}{\partial x} = G(y,t)$

Current density equation: $J(x,y,t) = q\mu n(x,y,t)\, E_x(y)$

Generation rate: $G(y,t) = \alpha\, \phi(t)\, e^{-\alpha y}$

Coordinate transformation:

$$\xi = \frac{1}{2}\left(t + \frac{x}{v}\right) \qquad \eta = \frac{1}{2}\left(t - \frac{x}{v}\right)$$

Analytical formulation is successfully obtained.

Photocurrent:

$$I(t) = \alpha\, qW \int_0^{\infty} dy \int_{t-L/v}^{t} dt' \mu_p |E_x(y)| e^{-\alpha y} \phi(t')$$

VI. Measurement System

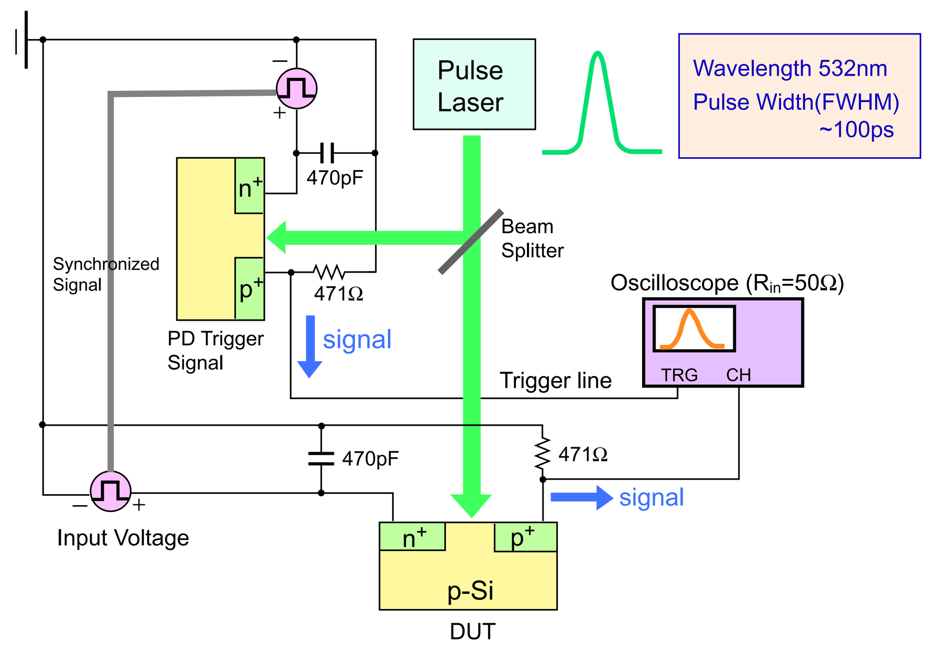

VII. Photodiode Modeling Results (1)

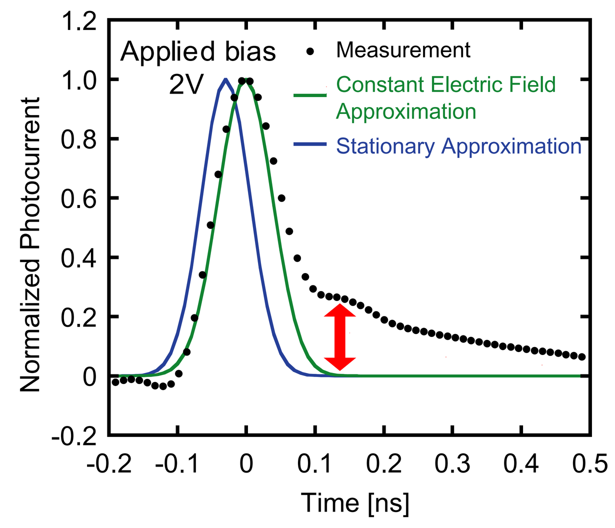

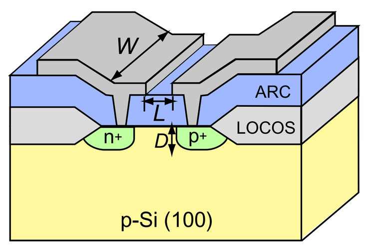

L = 2 μm
W = 100 μm
D = 0.5 μm
n+,p+ ~10^{20} cm^{-3}
Substrate ~10^{15} cm^{-3}

The general profile of the measured pulse is reproduced but the end tail can not be predicted.

VIII. Analysis of Electric Field

Approximation

$$E_x(y) = E_0 \exp\left(-\frac{y^2}{D^2}\right)$$

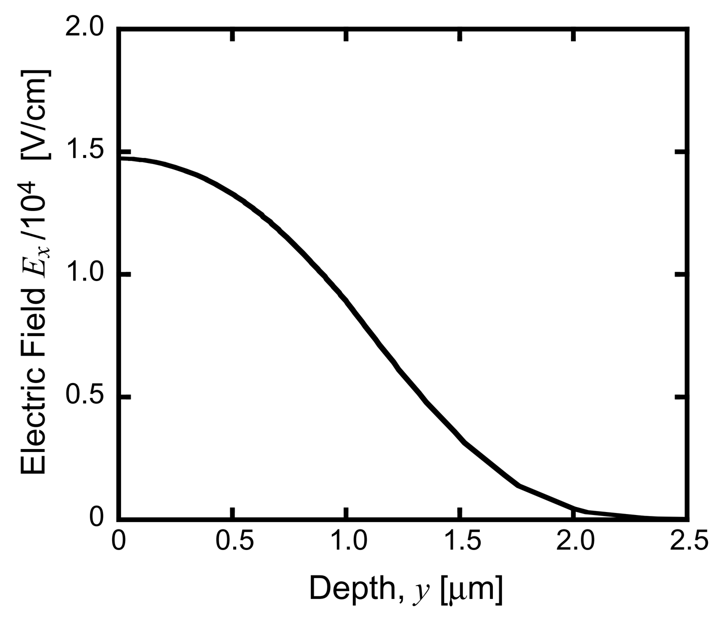

IX. Photodiode Modeling Results (2)

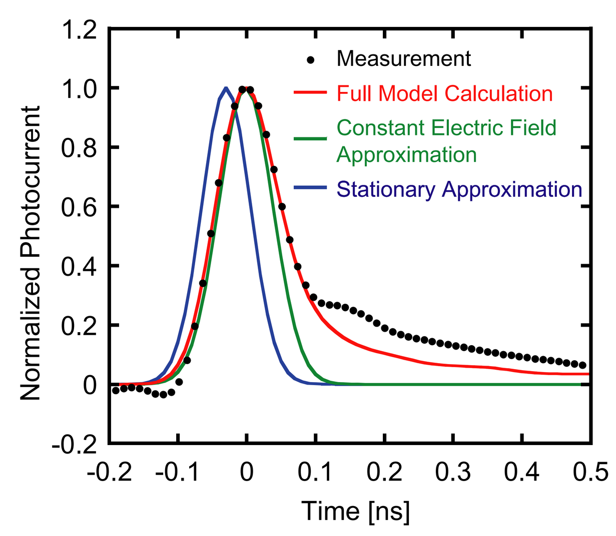

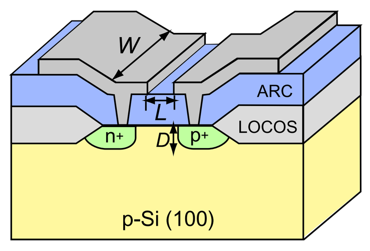

L = 2 μm
W = 100 μm
D = 0.5 μm
n+,p+ ~10^{20} cm^{-3}
Substrate ~10^{15} cm^{-3}

The full model calculation reproduces the end tail.

X. Application to Circuit Simulation

Transient Test Circuit

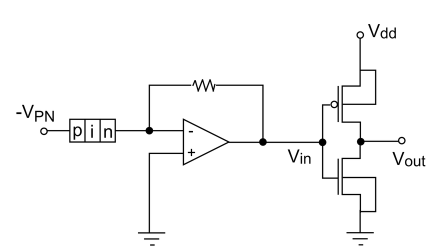

p-i-n photodiode equivalent circuit

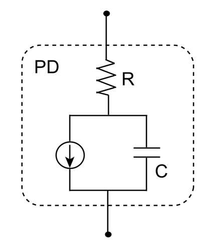

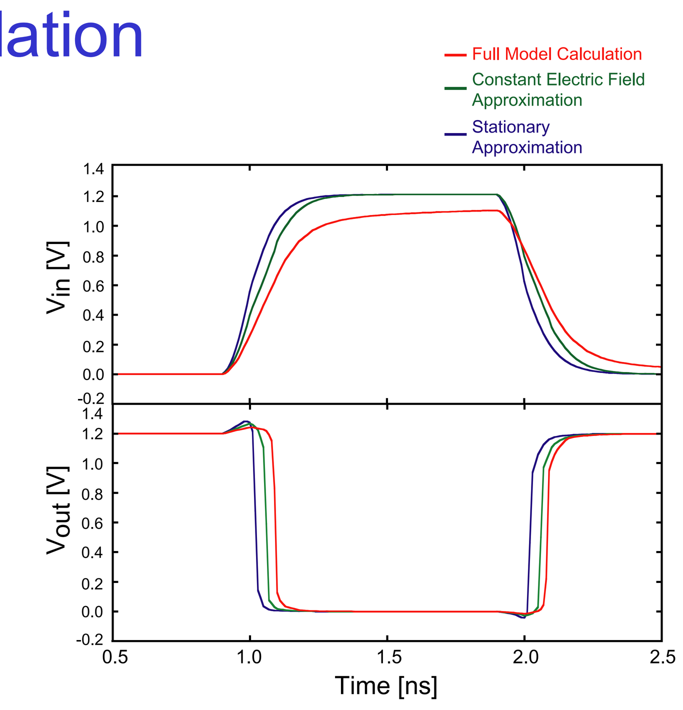

The test circuit output shows the delay predicted by the full model calculation.

Summary

- A time-domain model of the carrier transport in lateral p-i-n photodiode has been developed.
- The developed model accurately predicts photodiode current response down to ~100ps input pulse.
- We have demonstrated the effect of the photodiode response delay in a conventional transient inverter circuit.